Coupling of confined impurity states in doped double-quantum-well structures

Radha Ranganathan, B. D. McCombe, N. Nguyen, Y. Zhang, and M. L. Rustgi
State University of New York at Buffalo, Buffalo, New York 14260

W. J. Schaff
Cornell University, Ithaca, New York 14853
(Received 30 April 1991)

Far-infrared magnetotransmission investigations have revealed coupling effects on hydrogenic impurity states in doped GaAs/Al$_{0.3}$Ga$_{0.7}$As coupled double quantum wells. Impurity transitions of the well-center donors were measured in several samples with identical well widths but different narrow barrier widths. Results agree with variational calculations for all samples when intersubband mixing and the difference in the masses in the well and barrier are taken into account. Evidence for intersubband mixing in double wells is also provided.

Semiconductor quantum-well systems provide elegant illustrations of elementary quantum mechanics and are also technologically important. The simplicity of the problem is afforded by the use of the effective-mass approximation (EMA). Shallow impurities in bulk semiconductors have been successfully approximated by a hydrogenic model in the EMA. The bound levels of the donor electron are completely analogous to those of the free hydrogen atom, with the mass replaced by the effective mass (equals $0.067m_0$, for GaAs where m_0 is the free-electron mass) and including the dielectric constant of the host semiconductor (equals 12.5, for GaAs). The bound-level transition energies lie in the far infrared and can be measured as a function of externally applied magnetic fields (rydberg for GaAs $\mathcal{R} = 5.83$ meV, requiring modest magnetic fields to achieve the high-field limit). The shallow donor in a quantum well is then the problem of the hydrogenic atom in external potentials. Recent studies of shallow donors in isolated quantum-well structures in the GaAs/Al$_x$Ga$_{1-x}$As system[1] have explored the effects of confining potentials; results are in good agreement with variational calculations based on the one-band EMA with simple matching conditions on the envelope functions at the boundaries. The theoretical results were shown to be relatively insensitive to the choice of boundary conditions (BC) for this system.[2] In the study of coupled quantum-well systems where barrier penetration becomes important, one must recognize explicitly that the barrier and well materials are different; such coupled systems thus represent an extension of elementary quantum mechanics to real material systems. For narrow barrier systems or short period superlattices, the problems include the applicability of the EMA (valid for potentials varying slowly on the scale of the underlying lattice), a proper treatment of the BCs and the question of the barrier effective mass at the tunneling energy, which might be well below the conduction band edge. It is necessary to know what quantities are continuous across an interface and how the material parameters enter into the BCs.[3-6] The problem is thus of fundamental interest and also important in devices that rely on transport in the direction of the quantum wells.

The doped coupled double quantum well (CDQW) has been chosen in the present work as the simplest case for study where coupling can be observed directly. A CDQW structure consists of two quantum wells separated by a narrow barrier region. In a doped CDQW barrier, penetration is expected to produce the interesting effect of lowering the binding energy of the donor electron from that in a corresponding isolated quantum well and we present this observation. A significant aspect of our work is the observation of the effect of mixing of the two lowest (symmetric and antisymmetric) confinement states of the CDQW. Intersubband (ISB) mixing implies the presence of parity-breaking internal fields. We provide clear evidence for the importance of a proper accounting of coupling and ISB mixing in this paper. Additionally, the effect of interface BCs is also studied and found to be significant. Excitonic states and electric field effects in CDQWs have been investigated by photoluminescence[7-9] (PL) and intersubband resonances measured in the far infrared,[10] while to our knowledge no work has been reported on the study of impurity levels in the far infrared in doped CDQWs.[11] The sensitivity with which the donor level transitions can be measured makes far-infrared spectroscopy a superior tool to study the various approximation methods. Also the relative ease in dealing with the conduction band is an advantage in the analysis of shallow-donor level transitions as compared to interband excitonic transitions in which the complex valence-band states are involved.

In order to observe the coupling effect in a CDQW the ground state ($m = 0$) to first excited state ($m = +1$) transition of the confined hydrogenic shallow donor in a magnetic field is studied for various interwell barrier widths. Results show clearly that the transition energies decrease systematically with decreasing narrow barrier widths. The experimental results are compared with a variational calculation within the EMA. Excellent agreement is obtained. The calculation takes into account the ISB mixing and the difference in the barrier and well effective masses through the BC.

The samples investigated in this work are GaAs/Al$_{0.3}$Ga$_{0.7}$As quantum wells grown by molecular-beam epitaxy on GaAs buffer layers on semi-insulating GaAs substrates. All samples comprised twenty symmetric pairs
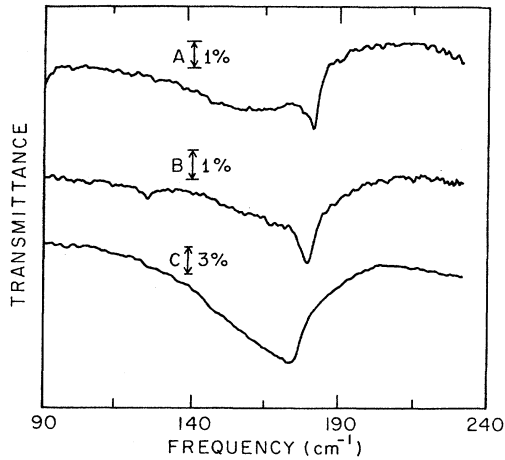
FIG. 1. Far-infrared transmission spectra at 9 T and 4.2 K of three CDQWs with interwell barrier widths of A, 48 Å; B, 18 Å; C, 9 Å. The full scale of the ordinate is 10% for A and B, and 20% for C.

of GaAs wells, each 170-Å wide separated by a thin $Al_{0.3}Ga_{0.7}As$ barrier (A, 48 Å; B, 18 Å; C, 9 Å). The coupled pairs are separated by 125-Å wide $Al_{0.3}Ga_{0.7}As$ barriers. This structure is clad on both sides by thick (1500–2000 Å) $Al_{0.3}Ga_{0.7}As$ layers. The central one-third region of each well is doped with silicon (A and B 1×10^{16} cm^{-3}; C 3×10^{16} cm^{-3}).

Far-infrared (80–250 cm^{-1}) transmission measurements were carried out with a Bomem DA3.02 Fourier-transform spectrometer in conjunction with a Ge:Ga photoconductive detector. The sample was mounted in the Faraday geometry with the applied magnetic field normal to the quantum well layers in helium exchange gas and placed in a 9 T superconducting magnet. Conventional light pipe optics and condensing cones are used to focus the far-infrared radiation onto the sample and couple with the spectrometer.

Results of magnetotransmission at 9 T are displayed in Fig. 1. The traces are ratios of the transmission spectra at 9 T to that at 0 T. The resolution is 1 cm^{-1}. The coupling effect is manifest as a decrease in the ground state ($m = 0$) to the first excited state ($m = +1$) transition energy with decreasing interwell barrier width. The increased absorption strength of the line for sample C is due to the larger doping density in this sample, and the strong tail to low frequency is due to the distribution of the impurities along the growth direction and the strongly modified wave function in this direction.[12] The magnetic field dependence of the transition energy for all three samples is plotted in Fig. 2. The 48-Å barrier in sample A produces minimal coupling, and the wells behave nearly as isolated wells as inferred from the data on impurities in single wells.[1] Coupling effects become measurable at a barrier width of 18 Å (sample B); the impurity transition energy shifts down by 3 cm^{-1} from that in a corresponding isolated well. Sample C (9-Å barrier) produces a shift of about 10 cm^{-1}. The uncertainty of about 5% in the well and barrier widths, determined from fits to

reflectivity spectra, leads to an uncertainty of less than ± 2 cm^{-1} in the transition energy.

Calculations of the transition energies for the samples studied were performed with a variational approach similar to the one adopted by Greene and Bajaj for isolated quantum wells.[2] Calculations are performed for a well-center impurity. There is no diffusion of donors at the growth temperatures. There is a redistribution along the growth direction. Nevertheless, because of the peak in the density of states at or near the center of the wells, a sharp peak corresponding to the impurity located at the center of the well is always observed.[12] The Hamiltonian in dimensionless units for a donor electron in a quantum well subjected to an external magnetic field B in the notation
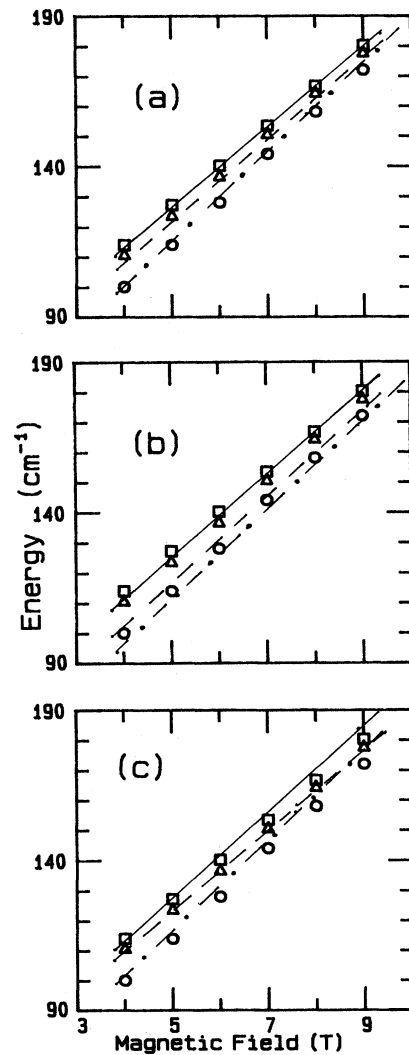
FIG. 2. The measured (symbols) and calculated (lines) hydrogenic donor transition energies vs B, for A, □ (———); B, △ (---); C, ○ (-·-·-). Calculations are with (a) inclusion of ISB mixing and the BC of continuity of $(1/m_e^*)df/dz$; (b) noninclusion of ISB mixing but BCs same as in (a); and (c) ISB mixing included but BCs of continuity of $f(z)$ and df/dz.

of Ref. 2 is

$$H = (m^*/m_e^*)(-\nabla^2 + \gamma L_z + \gamma^2\rho^2/4) - 2/r + V(z).$$

The origin of coordinates is chosen to be the midpoint of the interwell barrier. The position of the electron is $r = [\rho^2 + (z - z_i)^2]^{1/2}$, where ρ is the distance in the x-y plane and z_i denotes the z coordinate of the impurity; $\gamma = \hbar\omega_c/2\mathcal{R}$, $\omega_c = eB/m^*c$, where m^* is the effective mass in GaAs and m_e^* is the effective mass in a given region ($m_e^* = m^*$ in GaAs); L_z is the z component of the angular momentum in units of $\hbar$, and energy is in units of the effective rydberg, $\mathcal{R} = m^*e^4/2\varepsilon_0^2\hbar^2$, where ε_0 ($= 12.5$) is the static dielectric constant assumed to be the same in both the well and barrier. The potential $V(z)$ is given by

$$V_{(z)} = \begin{cases} V_0, & |z| < w/2 \text{ and } |z| > L + w/2, \\ 0, & w/2 < |z| < L + w/2, \end{cases}$$

where L is the width of each of the wells, and w is the thickness of the interwell barrier. The height of the potential due to the interwell barrier and semi-infinite external barriers, V_0, was taken to be 230 meV (given by the conduction-band discontinuity which is about 60% of the band gap difference[13]). Interaction between two impurities in a well can be neglected because at the doping levels ($\approx 5\times10^9$ cm^{-2}) in the sample the interimpurity spacing is ≈ 1400 Å (greater than the Bohr radius). The total energy was calculated variationally with the electron wave function approximated in terms of Gaussian basis sets,

$$\psi = f(z)\rho^{|m|}e^{im\phi}\sum A_{ij}\exp[-\alpha_i(z - z_i)^2]$$
$$\times \exp[-(\alpha_j + \beta)\rho^2]. \tag{1}$$

The set of parameters α_i used are given in Table I of Ref. 2. The parameters A_{ij} and β are determined variationally. The number of basis functions was restricted by requiring $A_{ij} = 0$ for $(i - j) > 1$. As in Ref. 2, the number of basis functions used for the ground state ($m = 0$) is 13, and that for the odd-parity states ($m = \pm 1$) is 10. The envelope function $f(z)$ in Eq. (1) is taken to be a linear combination of the two lowest subbands which correspond to the solutions of the Schrödinger equation with the potential $V(z)$ and without the Coulomb potential. The boundary conditions on the subband envelope functions are the continuity of $f(z)$ and the probability current, proportional to $(1/m_e^*)(\partial f/\partial z)$, at the interfaces, thus including the difference in the effective mass in the matching conditions. The values used were $m_e^* = 0.067m_0$ for GaAs and $0.0919m_0$ for Al$_{0.3}$Ga$_{0.7}$As.

The energies of the ground state, and the first excited state with $m = -1$ associated with the first symmetric subband were calculated variationally; the energy of the first excited state with $m = +1$ is obtained by adding 2γ, the cyclotron energy, to the $m = -1$ state. The latter energy is determined experimentally over the range of magnetic fields investigated; thus the problem of the nonparabolicity correction for the effective mass in the calculation is circumvented. A comparison of the experiment and calculation is shown in Fig. 2(a). Very good agreement,

within the experimental uncertainties, is obtained for all three samples. The Coulomb potential and the quantum well localize the electron in either one well or the other (Bohr radius ≤ 100 Å). The impurity doping density is sufficiently dilute that a particular impurity is not influenced by the effect of an impurity in the second well, and the donor may be treated as isolated in one well of the CDQW. Thus there is asymmetry and the states do not have definite parity.[14,15] The consequence of mixing the symmetric and the antisymmetric subband is to further localize the electron, thereby increasing the binding energy. Therefore if mixing is not included in the calculation, the transition energy is underestimated. A comparison between Figs. 2(a) and 2(b) illustrates this point. The lines in Fig. 2(b) are a result of the calculation with no mixing included and the subband envelope function ($f(z)$) is taken to be the symmetric subband alone. The most obvious disagreement in Fig. 2(b) is for the intermediate barrier (18 Å) width sample. The agreement is enormously improved when mixing is included [Fig. 2(a)]. In the limit of narrow interwell barriers where the splitting is large, the energy of mixing is also large, and therefore not favored. The 9-Å barrier sample, for which the splitting is ≈ 6 meV, belongs nearer this limit, and the improvement in the agreement when ISB mixing is included is small but noticeable. In the opposite limit of wide barrier widths the two levels are degenerate and are mixed in equal proportions. The resulting wave function is localized in one well and the binding energy is the same as for an isolated well. For the 48-Å barrier case when no mixing is included the agreement with the data is still good because the well and barrier widths are such that the hydrogenic part of the wave function decays sufficiently, so rapidly that the overall probability of the electron in the other well is small enough to render the contribution unimportant [see Eq. (1)]. However, for $W = 18$ Å, where the splitting is ≈ 3 meV, noninclusion of mixing causes the binding energy to be greatly underestimated.

Finally, we present a discussion of the BCs. The generally applicable boundary conditions for heterostructure systems are complex,[5,6] and we used a simplified version that is satisfactory for the material system studied. Calculations were also performed with the barrier and well masses set equal to the mass in GaAs. The BCs on the envelope function are then simply the continuity of $f(z)$ and its derivative. A comparison of the results is shown in Fig. 2(c). Taking the mass difference into account in the BCs increases the zero field transition energy and decreases the slope thus improving the agreement with the data over the entire field region (the correction to the transition energy then depends on the field). An important point that should be noted is that the decrease in slope, implying a heavier effective mass, is not due to nonparabolicity but rather a result of a better accounting of barrier electronic properties through the boundary condition.

In conclusion, coupling effects on confined impurity states have been observed. The experimental results are in very good agreement with the variational calculations. The results provide evidence in favor of intersubband mixing and the impact of boundary conditions that recognize the differences in the effective masses.

---

[1] A. A. Reeder, J.-M. Mercy, and B. D. McCombe, IEEE J. Quantum Electron. **24**, 1690 (1988), and references therein.

[2] R. L. Greene and K. K. Bajaj, Phys. Rev. **31**, 913 (1985).

[3] C. Priester, G. Allan, and M. Lannoo, Phys. Rev. B **28**, 7194 (1983).

[4] C. Mailhiot, Y-C. Chang, and T. C. McGill, Phys. Rev. B **26**, 4449 (1982).

[5] G. Bastard, Phys. Rev. B **24**, 5693 (1981).

[6] G. Brozak, E. A. de Andrada e Silva, L. J. Sham, F. DeRosa, P. Miceli, S. A. Schwarz, J. P. Harbison, L. T. Florez, and S. J. Allen, Jr., Phys. Rev. Lett. **64**, 471 (1990).

[7] Y. J. Chen, E. S. Koteles, B. S. Elman, and C. A. Armiento, Phys. Rev. B **36**, 4562 (1987).

[8] S. Charbonneau, M. L. W. Thewalt, E. S. Koteles, and B. Elman, Phys. Rev. B **38**, 6287 (1988).

[9] W. Xinghua and R. Laiho, Superlatt. Microstruct. **5**, 79 (1989).

[10] A. Lorke, A. D. Wieck, and U. Merkt, Superlatt. Microstruct. **5**, 279 (1989).

[11] T. Duffield, R. Bhat, M. Koza, M. C. Tamargo, J. P. Harbison, F. DeRosa, D. M. Hwang, P. Grabbe, and S. J. Allen, Jr., Solid State Commun. **60**, 557 (1986). The superlattice samples studied in this work contain a uniform distribution of impurities. The impurity transition lines are broad and do not lend themselves to a simple analysis.

[12] J.-M. Mercy, B. D. McCombe, W. Beard, J. Ralston, and G. Wicks, Surf. Sci. **196**, 334 (1988).

[13] G. Duggan, H. I. Ralph, and K. J. Moore, Phys. Rev. B **32**, 8395 (1985).

[14] I. Galbraith and G. Duggan, Phys. Rev. B **40**, 5515 (1989).

[15] T. Kamizato and M. Matsura, Phys. Rev. B **40**, 8378 (1989).